Supporting Information: Effect of solvent polarity and electrophilicity on quantum yields and solvatochromic shifts of single-walled carbon nanotube photoluminescence

Brian A. Larsen,[1] Pravas Deria,[2] Josh M. Holt,[1] Ian N. Stanton,[2] Michael J. Heben,[3] Michael J. Therien,[2] and Jeffrey L. Blackburn[1]

[1]Chemical & Materials Science Center, National Renewable Energy Laboratory, 1617 Cole Boulevard, Golden, CO 80401

[2]Department of Chemistry, French Family Science Center, 124 Science Drive, Duke University, Durham, NC 27708

[3]Department of Physics and Astronomy, Wright Center for Photovoltaics Innovation and Commercialization, The University of Toledo, Toledo, OH 43606

S-1: Characterization of SWCNT-PNES conformation and interaction

The helical wrapping of SWCNT-PNES is depicted in Figure S-1. In our previous work, we observed this helical conformation by TEM and AFM with a measured periodicity of ~10 nm independent of SWCNT-PNES solvent (1). The observations from microscopy are supported by elemental analysis of the SWCNT-PNES materials, which possess a 1:1:27 ratio of S:Na:C. This ratio of S:Na:C is consistent with the expected PNES:SWCNT ratio, assuming a helicial PNES periodicity of 10 nm and a SWCNT average diameter of 1 nm.

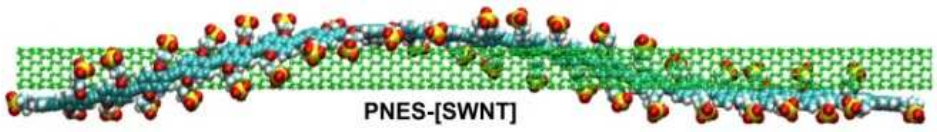

Figure S1 – The helical conformation of PNES-SWCNT is illustrated here showing the 10 nm periodicity of the PNES helical wrapping around a 1 nm diameter SWCNT with accurate proportional scale.

We also find the PNES-induced strain of the SWCNT to be unchanged in the different solvents based on equivalent RBM Raman shifts and relative intensities (2) for each PNES-SWCNT/solvent system (Figure S2 and Table S1).

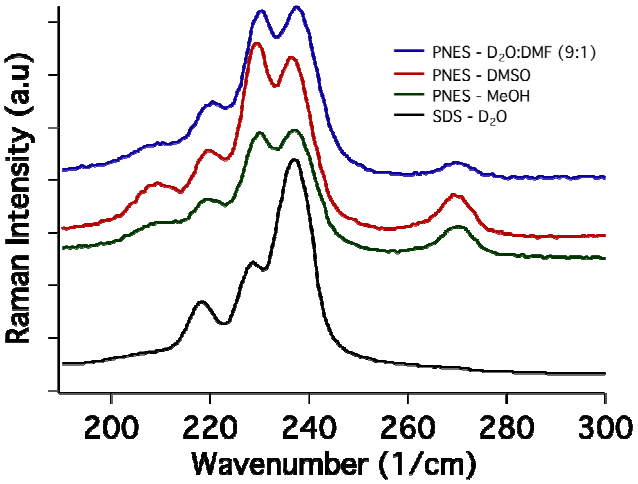

Figure S2: RBM spectra of PNES-SWCNTs in D2O:DMF (9:1), DMSO, and MeOH relative to that of SDS-coated tubes (black spectra) in D_2O taken at room temperature, λ_{ex} = 785 nm.

Table S1: RBM frequencies of various SWNTs wrapped with PNES in different solvents relative to that of SDS-coated tubes in D_2O; experimental condition: room temperature, λ_{ex} = 785 nm. These data show ~2-3 cm^{-1} higher-energy shift of these RBM frequencies for PNES-wrapped SWCNT compared to that of surfactant coated SWCNT.

SWNT (n,m)	SDS-D_2O Shift (cm^{-1})	PNES-D_2O Shift (cm^{-1})	PNES-DMSO Shift (cm^{-1})	PNES-MeOH Shift (cm^{-1})
(13,3)	205	208	209	209
(9,7)	218	220	219	219
(10,5)	228	230	229	230
(12,1)	237	238	237	238
(10,2)	269	270	270	270

S-2: Optical spectroscopy of PNES-SWCNT

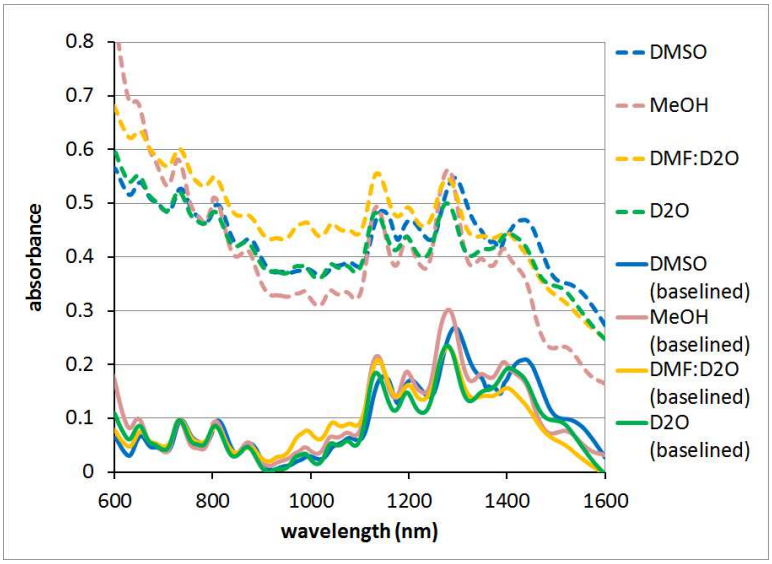

Figure S2 - The absorption spectra of each sample, measured using a 1 cm path length. The baselined spectra have been determined by subtracting an inverse power law fit of the background absorbance each spectrum. The ratios of the S11:S22 absorption areas are 6.2, 6.0, 5.4, and 5.2 for DMSO, methanol, 9:1 D_2O:DMF, and D_2O, respectively.

Estimation of Inner Filter Effects

PLE measurements were performed in front face configuration specifically to minimize problems with inner filter effects. However, these effects, while minimized, cannot be completely eliminated for the solvents used in this study. In particular, the photoluminescence of an (8,6) SWCNT may be attenuated by both methanol and DMSO, as both possess absorption bands near the (8,6) E_{11} (1176 nm). To estimate the inner-filter effects of methanol and DMSO, the PL intensity of a standard D_2O dispersion of SWCNTs was measured as a function of cuvette path length (t), using 0.1, 0.2, 0.5, and 1.0 cm path length cuvettes. Relative to a 1.0 cm cuvette, the PL intensity observed from a 0.1 cm cuvette is 74% and a 0.2 cm is 98%, which indicates that the "active" path length of the front face geometry giving rise to the collected emission intensity is the first 0.2 cm of the cuvette.

At 1176 nm (the E_{11} transition for the (8,6) SWCNT), the optical density of the DMSO is 0.6, while that of the methanol is 0.4 (in a 1 cm cuvette). This equates to extinction coefficients, α, of 1.39 cm^{-1} and 0.92 cm^{-1} for DMSO and methanol, respectively, in the equation $T=e^{-\alpha t}$. We then calculate the relative number of photons collected as a function of depth within the first 0.2 cm of the cuvette for each solvent using:

(1) an optical density of 0.5 (1 cm cuvette, α=1.15 cm^{-1}) for the (8,6) S_{22} transition determining the relative number of photons absorbed in both cases and (2) the associated extinction coefficients for DMSO and methanol determining the number of emitted photons that are reabsorbed by the inner filter effect. This calculation allows us to estimate that the increased absorbance of the DMSO absorption band leads to a reduction of ~4.2% in the number of photons collected from the (8,6) SWCNT in the DMSO sample relative to the methanol sample. Thus, a correction for this inner filter effect would increase the relative quantum yield of the (8,6) SWCNT in DMSO slightly, by ~4%, relative to methanol. Since this effect is small, and does not affect any conclusions from the manuscript, we do not adjust the QY values reported in the manuscript for minor inner filter effects.

S-3: A comparison of relative SWCNT photoluminescence (PL) quantum yields vs. solvent donor number.

The donor number reflects the electron donating character of the solvent (3).

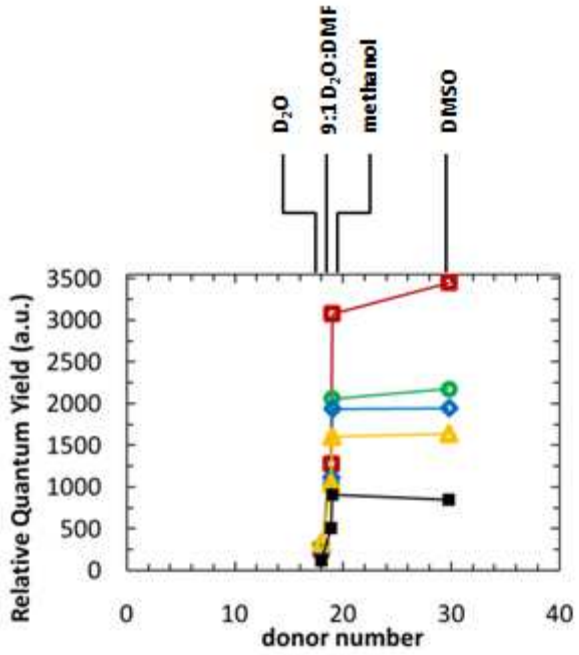

Figure S3 –SWCNT PL quantum yield vs. solvent donor number (DN) follows a reverse relationship compared to the solvent acceptor number (AN). The solvents used in this study have very similar DN, resulting in a much closer spacing of data points than comparing SWCNT PL quantum yield vs. AN (DN = 18, 18.9, 19, and 29.8 and AN=54.8, 53.2, 41.3, and 19.3 for D_2O, 9:1 D_2O:DMF, Methanol, and DMSO, respectively).

S-4: Detailed description of equation for estimating Eii, vac

The following equation is used to interpolate optical transition energies (E_{ii}) of SWCNT and was originally developed by Bachilo et al. (4):

$$E_{ii,Vac} = \frac{1241}{A_1 + A_2 \cdot d} + A_3 \cdot \frac{cos(3\theta)}{d^2} \qquad \text{Equation S1}$$

The A_1, A_2, and A_3 parameters were fit by Choi and Strano (5) using SWCNT E_{ii} data from studies with dielectric environments similar to vacuum ($\varepsilon \sim 1$). To calculate E_{11} energies, the parameters A_1 and A_2 are 61.1 nm and 1113.6. The value of A_3 depends on the SWCNT (n,m) chirality. For j=mod[(n-m), 3], A_3 is -0.077 if j=1; A_3 is 0.032 if j=2. To calculate E_{22} energies, the parameters A_1 and A_2 are 87.4 nm and 613.7. The value of A_3 depends on the SWCNT (n,m) chirality. For j=mod[(n-m), 3], A_3 is 0.143 if j=1; A_3 is -0.191 if j=2. Lastly, θ and d are the chiral angle and diameter, respectively, of each SWCNT (n,m) species.

S-5: Relative magnitude and diameter dependence of SWCNT solvatochromic shifts: E_{11} vs. E_{22}

The differences in the diameter dependent Stark effects for E_{11} and E_{22} (magnitude and slope) can be understood by considering the effect of a changing dielectric constant on both of the many-body Coulomb interactions: the exciton binding energy (E_{bd}) and the self-energy (Σ). The former is the attractive electron-hole Coulomb interaction and the latter is the repulsive electron-electron interaction. The exciton energy (E_{exc}) is the sum of the single-particle excited state energy that can be calculated by simple tight-binding (E_{TB}) and many-body Coulomb interactions:

$$E_{exc} = E_{TB} + \Sigma - E_{bd} \qquad \text{Equation S2}$$

In Equation S2, the self-energy is a repulsive energy, and is therefore positive, while the binding energy is attractive, and is therefore negative. Both Σ and E_{bd} are proportional to the effective masses of the carriers involved. E_{bd} is determined by the effective mass of an electron at the bottom of the conduction band (CB) and a hole at top of the valence band (VB). In contrast, Σ is determined by the effective mass of an electron at the bottom of CB and of an electron *near* the top of the VB. Since the effective mass of electrons in VB increase with increasing k, the effective mass of the VB electron is larger than that of the thermalized VB hole. This larger effective mass means that the self-energy term Σ is always larger than the E_{bd} term. Placing $\Sigma > E_{bd}$ into Equation S2 implies that the exciton energy will always be larger than the single-particle excited state energy calculated by tight binding.

When considering the implications of Equation S2 on the solvatochromic shift, we first note that solvatochromism results from the local screening of Coulomb interactions by adjacent solvent molecules. Increasing the dielectric constant ε screens the Coulomb interactions for both repulsive e-e interactions (Σ) and for attractive e-h interactions (E_{kb}). Since Σ is always larger than E_{bd}, the magnitude of the decrease in Σ will be larger than the magnitude of the decrease in E_{bd} for a given dielectric constant ε: $|\Delta\Sigma| > |\Delta E_{kb}|$. Returning to Equation S2, this implies a reduction in the many-body term ($\Sigma - E_{bd}$), leading to a red-shift with increasing dielectric constant, or the solvent Stark effect.

The discussion above emphasizes that the important factor to consider for the E_{ii} diameter dependence of the solvatochromic shift is the many-body term ($\Sigma - E_{bd}$). Sato et al. have shown (Figure 8 of reference 7), that the many body term $|\Sigma - E_{bd}|$ is larger for E_{22} than it is for E_{11}, independent of diameter. This implies that the magnitude of the solvatochromic shift (ΔE_{11}) for the E_{22} should be slightly larger than that of the E_{11} for a given diameter, as observed. Figure 8 of the same reference also indicates that the many-body term for E_{22} rises more steeply than E_{11} as a function of decreasing diameter, barring some deviations for Type II SWCNTs at very small diameters. This implies a stronger diameter dependent slope for ΔE_{22} than for ΔE_{11}, with ΔE_{22} increasing more rapidly as a function of decreasing diameter.

S-6: Derivation of SWNT solvatochromism model

The SWNT solvatochromism model used in this work is was originally developed by Choi and Strano (5) and recently adapted by Silvera-Batista *et al* .(7). The solvatochromic shift of SWNTs is described by the following relationship (5):

$$\Delta E_{ii} = E_{ii,solvent} - E_{ii,Vac} = -L_{solvent}\frac{\Delta\alpha_{SWNT}}{\beta\gamma d^2}\Delta f_{solvent-Vac} \qquad \text{Equation S3}$$

Where E_{ii} is the SWCNT solvatochromic shift, $E_{ii,\,solvent}$ is the observed optical transition energy, $E_{ii,\,Vac}$ is the interpolated optical transition energy from Equation S1, $L_{solvent}$ is a parameter that reflects the polarization fluctuation within the Onsager volume, and is associated with solvent interactions with the SWCNT solute, α_{SWNT} is the polarizability change of a photoexcited SWNT relative to the ground state, β is a SWNT shape factor, γ is a spatial SWNT polarizability factor, d is the SWNT diameter, and $\Delta f_{solvent-Vac}$ represents the difference of the solvent polarity relative to vacuum.

We use the relationship empirically developed by Silvera-Batista *et al* to define $\Delta\alpha_{SWNT}$ as the polarizability of the exciton (Eq. S4) (7), and we define $\Delta f_{solvent\text{-}air}$ using the difference of the Onsagar polarity functions (Eq. S5):

$$\Delta\alpha_{SWNT} = k \cdot d^{-2} \cdot E_{ii}^{-3} \qquad \text{Equation S4}$$

$$\Delta f_{solvent-air} = [f(\varepsilon) - f(\eta^2)]_{solvent} = \frac{2(\varepsilon-1)}{2\varepsilon+1} - \frac{2(\eta^2-1)}{2\eta^2+1} \qquad \text{Equation S5}$$

Where k is a proportional constant, ε is the solvent dielectric constant, and η is the solvent index of refraction. We note that because the solvents in this study are polar, we used the difference of the Onsager polarity functions in Eq. S5 to most accurately describe the polarizable-polar interactions of the photoexcited SWNT and solvent molecules(8).

Substituting Equations S4 and S5 in Equation S3 yields the following expression:

$$\Delta E_{ii} = -L_{solvent} \frac{k \cdot R^{-2} \cdot E_{ii}^{-3}}{\beta\gamma d^3} [f(\varepsilon) - f(\eta^2)]_{solvent} \qquad \text{Equation S6}$$

Algebraic manipulation of Equation S6 and consolidation of the proportional constants yields Equation S7, the expression used in our study:

$$\Delta E_{ii} E_{ii,Vac}^3 = -D_{SWNT \cdot solvent} \cdot [f(\varepsilon) - f(\eta^2)]_{solvent} \cdot \frac{1}{d^3} \qquad \text{Equation S7}$$

Where $-D_{SWNT \cdot solvent} = C_{SWNT} \cdot L_{solvent}$ and $C_{SWNT} = k \cdot \beta^{-1} \cdot \gamma^{-1}$

S-7: Linear regression statistics of SWNT-PNES/solvent data

For ΔE_{11} fits, $R^2 = 0.998$, 0.995, 0.997, and 0.999 for the E_{11} data of SWNT-PNES in methanol, DMSO, D2O, and 9:1 D_2O:DMF, respectively. For ΔE_{22} fits, $R^2 = 0.977$, 0.980, 0.974, and 0.972 for methanol, DMSO, D_2O, and 9:1 D_2O:DMF, respectively. We note that the regression was constrained to the relationship y = mx as opposed to y=mx + b, as the former linear equation correctly describes the SWNT solvatochromism model of Equation 1, since the offset parameter "b" in the latter equation has no physical basis.

An independent sample unequal variance t-test indicates that $-m_{methanol}$ and $-m_{DMSO}$ are statistically indistinguishable, as the data fail to reject the null hypothesis that the two linear regression slopes are identical (p = 0.27). The same test returns p=0.47 for $-m_{D2O}$ and $-m_{9:1\ D2O:DMF}$. The t-statistic (t) and

degrees of freedom (d.f.) were calculated for each SWNT-PNES/solvent data set using Equations S8 and S9(9):

$$t = \frac{m_{solvent\ 1} - m_{solvent\ 2}}{\sqrt{SE^2_{solvent\ 1} + SE^2_{solvent\ 2}}} \quad \text{(S8)}$$

$$d.f. = \frac{\left(SE^2_{solvent\ 1} + SE^2_{solvent\ 2}\right)^2}{\frac{SE^4_{solvent\ 1}}{n_{solvent\ 1}-1} + \frac{SE^4_{solvent\ 2}}{n_{solvent\ 2}-1}} \quad \text{(S9)}$$

Where m is the calculated regression slope, SE is the standard error of the linear regression, and n is the number of data points used in the linear regression.

S-8: PNES-SWCNT E_{ii} data

SWCNT	DMSO		Methanol		9:1 D_2O:DMF		D_2O	
(n,m)	E_{22} (nm)	E_{11} (nm)	E_{22} (nm)	E_{11} (nm)	E_{22} (nm)	E_{11} (nm)	E_{22} (nm)	E_{11} (nm)
(6,5)	563	973	568	978	-	-	-	-
(7,5)	650	1029	646	1025	658	1037	658	1037
(7,6)	650	1122	649	1121	661	1133	658	1130
(8,3)	671	958	664	951	-	-	-	-
(8,4)	593	1115	592	1114	604	1126	601	1123
(8,6)	722	1177	721	1176	730	1185	727	1182
(8,7)	734	1271	-	-	742	1279	739	1276
(9,4)	728	1107	724	1103	733	1112	733	1112
(9,5)	-	-	-	-	691	1260	688	1257
(9,7)	803	1332	799	1328	-	-	-	-
(9,8)	815	1416	814	1415	-	-	-	-
(10,2)	743	1059	742	1058	-	-	-	-
(10,3)	643	1260	640	1257	646	1263	649	1266
(10,5)	794	1255	793	1254	802	1263	-	-
(10,6)	767	1390	763	1386	-	-	-	-

References

(1) Deria, P.; Sinks, L. E.; Park, T. H.; Tomezsko, D. M.; Brukman, M. J.; Bonnell, D. a; Therien, M. J. *Nano Letters*. **2010**, *10*, 4192-4199.

(2) Cronin, S. B.; Swan, A. K.; Unlu, M.S.; Goldberg, B. B.; Dresselhaus, M. S.; and Tinkham, M. *Phys. Rev. B*. **2005**, *72*, 035425.

(3) Gutmann, V. *Electrochimica Acta*. **1976**, *21*, 661-670.

(4) Bachilo, S. M.; Strano, M. S.; Kittrell, C.; Hauge, R. H.; Smalley, R. E.; Weisman, R. B. *Science.* **2002**, *298*, 2361-2366.

(5) Choi, J. H.; Strano, M. S. *Applied Physics Letters*. **2007**, *90*, 223114.

(6) Sato, K.; Saito, R.; Jiang, J.; Dresselhaus, G.; Dresselhaus, M. S.; Phys. Rev. B. **2007**, *76*, 195446.

(7) Silvera-Batista, C. a; Wang, R. K.; Weinberg, P.; Ziegler, K. J. *Physical Chemistry Chemical Physics*. **2010**, *12*, 6990-8.

(8) Suppan, P. *Journal of Photochemistry and Photobiology A: Chemistry*. **1990**, *50*, 293-330.

(9) Welch, B. L. *Biometrika*. 1947, *34*, 28-35.